

# Simulation of the Formation of Beryllia Slurry

Uzak Zhabpasbayev<sup>\*1</sup>, Gaukhar Ramazanova<sup>2</sup>, Zamira Sattinova<sup>3</sup>, Ainash Shabdirova<sup>4</sup>

<sup>1, 2, 4</sup>Kazakh-British Technical University, 050000, Tole bi Street, 59, Almaty, Republic of Kazakhstan

<sup>3</sup>L.N. Gumilyev Eurasian National University, 010000, Munaitpasov Street, 5, Astana, Republic of Kazakhstan

<sup>\*</sup>u.zhabpasbayev@kbtu.kz; <sup>2</sup>gaukhar\_iz\_ram@mail.ru; <sup>3</sup>sattinova\_zamira@mail.ru; <sup>4</sup>ainash06@gmail.com

## Abstract

Simulation results of the formation process of the ceramic fabrications by a hot molding method are presented. Mathematical model describes motion and heat exchange of the liquid thermoplastic slurry of beryllia including the aggregate state change. Velocity and temperature fields during the formation process in the bushings with flat cavity have been obtained. Heat flow distribution at the wall of the form-building cavity is demonstrated. The increase of the slurry density during the transition from the liquid state into the viscous-plastic and solid-plastic states is defined. Comparison of the calculated data versus experimental data is presented.

## Keywords

*Thermoplastic Slurry; Formation Process; Solidification; Viscous-Plastic State; Solid-plastic State*

## Introduction

The method of hot molding includes motion and heat exchange of the slurry in the liquid state, as a solid-liquid mixture and a solid-plastic mixture. At stages of filling the form-building cavity and holding under pressure, it is very important to ensure a most structure destruction to obtain the homogeneous slurry, which is achieved by ultrasonic (US) exposure. Minimal friction upon walls of the form-building cavity and maximal plasticity must be reached during the solidification process, to avoid the destruction of the newly formed structure of the molding.

Hydrodynamics of thermoplastic slurry during molding relates to the class of the physical processes of flow and deformation. Slurry flow maintains its configuration after leaving the feeder. It was found during experiments, that for considered molding velocities, the flow of the thermoplastic slurry in the casting mould is laminar. The slurry arrives in the mold at the temperature of 75°C and cools down up to 45°C, at which the molding can be extracted from the mold without buckling.

Development and realization of the hot molding method mainly have an empirical nature, and the

detailed analysis on the motion and heat exchange will allow a comprehensive study on the ceramics formation process. Below, the modeling of the ceramics formation process of beryllia by hot molding method is presented.

## Rheological Model of the Thermoplastic Slurry

Thermoplastic slurry (high-viscous suspension) is a two-phase dispersed system, where solid mineral phase is beryllia powder (Table 1), and liquid phase is an organic binder. Organic binder consists of 3 components: paraffin, beeswax and oleic acid in the ratio of 0.82 : 0.15 : 0.03.

Beryllia powder has granulometric composition by fractions (Table 1). Mass fraction  $\omega = \frac{m_{bin}}{m_{ber} + m_{bin}}$  of organic binder normalized to unity is changed in the range of 0.095 – 0.117, where  $m_{bin}$  is the mass of binder and  $m_{ber}$  is the mass of beryllia powder.

TABLE 1 MAIN CHARACTERISTICS OF BERYLLIA POWDER

	Bulk weight $\rho_0 \times 10^3$ kg/m <sup>3</sup>	0.75
	Specific surface area, $S \times 10^3$ m <sup>2</sup> /kg	1.72
Granulometric composition by particle fractions of beryllia	Size, $\mu m$	Content, %
	up to 1.4	35.2
	1.4-4.2	52.7
	4.2-7.0	9.6
	7.0-9.8	1.7
	9.3-12.6	0.4
	12.6-15.4	0.3
	15.4-18.2	0.1

Molding properties of the slurry are satisfactory for this composition of the BeO powder (Table 1), if binder mass content is varied from  $\omega = 0.095$  to  $\omega = 0.117$ . The required amount of binder rises with increasing amount of finer fractions in the BeO powder, which worsens molding characteristics of the

slurry. An increase of the amount of coarser fractions in the BeO powder causes a coloring of ceramic, which is sign of presence of micro pores and fractures.

Thermoplastic slurry with thixotropic nature of flow can be related to viscous-plastic fluids of Shvedov-Bingham within the range of shear rate of 0.005–1200 s<sup>-1</sup>:

$$\tau = \tau_0 + \mu \frac{\partial u}{\partial y} \quad (1)$$

where  $\tau$  is shear stress;  $\tau_0$  is yield point;  $\mu$  is plastic viscosity coefficient,  $\partial u / \partial y$  is the change of the longitudinal velocity along  $y$  coordinate.

Ultrasonic exposure influences the rheological properties of the slurry. Plastic viscosity coefficient,  $\mu$ , and yield point,  $\tau_0$ , of the slurry depend on temperature,  $T$ , and mass fraction of the binder,  $\omega$ . The experimental data of  $\mu$  and  $\tau_0$  before ultrasonic exposure for the binder mass fraction  $\omega = 0.117$  are described by empirical dependences according to the experimental data of:

$$\mu(T) = 2.31 \cdot 10^9 \cdot \exp(-0.05816 \cdot T), (Pa \cdot s) \quad (2)$$

$$\tau_0(T) = 11.4 + 11.41 \cdot \exp\left(-\frac{T-343.05}{5.47}\right), (Pa) \quad (3)$$

and after 20 minutes ultrasonic exposure:

$$\mu(T) = 1.60 \cdot 10^{11} \cdot \exp(-0.07088 \cdot T), (Pa \cdot s) \quad (4)$$

$$\tau_0(T) = 18.1 + 8.3 \cdot \exp\left(-\frac{T-342}{4.8}\right), (Pa) \quad (5)$$

The temperature is defined in Kelvin's  $K$  in empirical dependences Eq.2 - 5.

Density of the thermoplastic slurry is defined by the concentration of the binder and densities of the beryllia powder and the binder:

$$\rho = \frac{\rho_{mb} \cdot \rho_{cb}}{(1-\omega)\rho_{cb} + \omega \cdot \rho_{mb}}, \left(\frac{g}{cm^3}\right) \quad (6)$$

where  $\rho_{mb}$  is the density of the beryllia,  $\rho_{cb}$  is the density of the binder,  $\omega$  is relative mass content of the binder normalized to unity.

Density of the binder dependent on the temperature is determined from empirical equation according to the experimental data:

$$\rho_{cb}(T) = 0.852 + 0.0725 \cdot \cos[\pi(0.01786 \cdot T - 5.3274)], \left(\frac{g}{cm^3}\right) \quad (7)$$

The density of the beryllia is  $\rho_{mb} = 3.02 \text{ g/cm}^3$ . The density of the binder  $\rho_{cb}$  in the range of temperature between 348K and 318K is changed within 0.7840 g/cm<sup>3</sup> and 0.8845 g/cm<sup>3</sup> in addition, the density of the thermoplastic slurry during solidification increases from 2.2643 g/cm<sup>3</sup> to 2.3548 g/cm<sup>3</sup>.

As it was determined experimentally, ultrasonic exposure has almost no influence on either thermal conductivity or thermal capacity. Both the thermal conductivity,  $\lambda$ , and thermal capacity,  $c_p$ , depend on the temperature in accordance with (8) and (9):

$$\lambda(T) = 7.1 \cdot \exp(-0.01 \cdot T + 2.73), (W/m \cdot K) \quad (8)$$

$$c_p(T) = 1000 \cdot \exp(0.00345 \cdot T - 0.94), (J/kg \cdot K) \quad (9)$$

Thus, rheological properties of the beryllia thermoplastic slurry are functions of temperature, and an aggregate transformation of liquid suspension into solid-plastic state during the forming process occurs.

### Mathematical Model

A flow and a heat exchange of thermoplastic slurry in a bushing are considered (Fig.1). The bushing has a form-building cavity of flat shapes (Fig. 1). The flat cavity (Fig. 1) has a thickness of  $2h = 0.0015 \text{ m}$ , a width of  $B=0.03 \text{ m}$  and a length of  $L=0.071 \text{ m}$ . The cooling contour of the bushing (Fig.1) is divided into 3 parts. Temperature of the cooling water in the first part is  $\theta_1 = 73^\circ\text{C}$ , in the second part -  $\theta_2 = 59^\circ\text{C}$ , in the third part -  $\theta_3 = 45^\circ\text{C}$  (Fig.1). The liquid slurry flows in the cavity with the initial temperature of  $\theta_0 = 75^\circ\text{C}$  (Fig.1). The mass of slurry is cooled and solidified during the movement. At the exit of the cavity, it becomes a structural form. Motion of the thermoplastic slurry is a laminar flow. The feature of the beryllia slurry is its high thermal conductivity; however Prandtl number  $Pr = \frac{\mu c_p}{\lambda}$  is much higher than unity due to high viscosity of the thermoplastic slurry. Density of the slurry is variable and increases with solidification.

The problem is studied in Cartesian coordinate system with axes of  $z$  and  $y$ . OZ axis coincides with the cavity axis direction, and OY axis is transverse directed to the cavity axis. Molding velocity is directed vertically downward along the axis OZ.

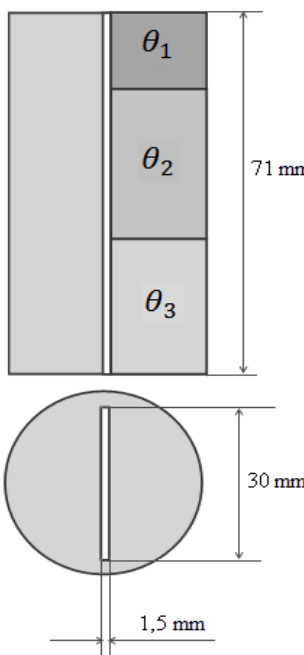


FIG. 1 BUSHING DIAGRAM OF A FLAT CAVITY

Transverse component of the velocity along the axis OY originates from the cooling of the liquid slurry on the side of the wall. An intensive circulation of water occurs in the cooling contours. Therefore wall temperature of each part of the cavity is believed to be equal to the temperature of the cooling fluid.

Rheological properties of the liquid slurry are changed as a result of solidification, and the heat of phase transition is released on the surface of the aggregate transition. Cooling of the slurry may lead to the irregularity of the temperature profile and rheological properties of the pressed out slurry. Solidification begins on the side of the wall, while the slurry may be in liquid state in the center of the cavity. As a result, replenishment by the liquid slurry for the compensation of internal volume shrinkage in the cooling zone of the cavity may occur.

The motion of the slurry is considered to be steady-state along the direction of the molding velocity and for its investigation a set of motion equations of non-Newtonian fluids involving the Shvedov-Bingham model for expression of  $\tau$  according to equation (1) is used:

$$\rho u \frac{\partial u}{\partial z} + \rho v \frac{\partial u}{\partial y} = - \frac{dp}{dz} + \frac{\partial}{\partial y} \left( \mu \frac{\partial u}{\partial y} \right) + \frac{\partial}{\partial y} (\tau_0) + \rho g \quad (10)$$

$$\frac{\partial \rho u}{\partial z} + \frac{\partial \rho v}{\partial y} = 0 \quad (11)$$

$$\rho u c_p \frac{\partial T}{\partial z} + \rho v c_p \frac{\partial T}{\partial y} = \frac{\partial}{\partial y} \left( \lambda \frac{\partial T}{\partial y} \right) + H_k \left( u \frac{\partial \rho}{\partial z} + v \frac{\partial \rho}{\partial y} \right) + \mu \left( \frac{\partial u}{\partial y} \right)^2 \quad (12)$$

The following notations are here used:  $z, y$  – axial and transverse coordinates;  $u, v$  – components of the velocity vector;  $p, \rho, T, \tau_0, c_p, \mu, \lambda$  - pressure, density, temperature, shearstress, coefficients of thermal capacity, viscosity and heat conductivity of the slurry, respectively.

Equations 10 – 12 describe the formation process in a flat cavity.

The heat of aggregate transition of the beryllia slurry found by experimental data is equal to  $H_k = 7800 \text{ J/kg}$ . Rheological properties of the slurry are expressed according to the previously mentioned empiric equations (2) - (9).

Condition of conservation of the mass flow rate permits to define a pressure gradient to press out thermoplastic slurry from the molding mold:

$$\int \rho u dS = \rho_0 u_0 S \quad (13)$$

where  $S$  is cross-section area of the cavity.

Both velocity and temperature distributions at the inlet are considered to be constant along the cross-section of the cavity and all the thermo-physical properties of the slurry are constant:

$$u = u_0, v = 0, T = \theta_0 \quad (14)$$

if  $z = 0$ .

Symmetry conditions are assumed at the cavity axis:

$$\frac{\partial u}{\partial y} = \frac{\partial T}{\partial y} = v = 0 \quad (15)$$

if  $z > 0, y = 0$ .

For the longitudinal velocity, the conditions of sticking and sliding are set at the wall, depending on the aggregate state of the slurry. It is assumed that the temperature of the cavity wall at each zone is maintained to be constant and equal to the temperature of the cooling fluid. Marking the water temperature in the first, second and third contours as  $\theta_1, \theta_2, \theta_3$ , respectively, the boundary conditions for the temperature at the wall are achieved:

$$T = \theta_1, u = 0 \quad (16)$$

if  $0 \leq z < l_1, y = y_1$ .

$$T = \theta_2, -\frac{dp}{dz} = \frac{1}{y_1} \left[ \tau_{0w} + \left( \mu \frac{\partial u}{\partial y} \right)_w \right] \quad (17)$$

if  $l_1 \leq z < l_2, y = y_1$ .

$$T = \theta_3, -\frac{dp}{dz} = \frac{1}{y_1} \left[ \tau_{0w} + \left( \mu \frac{\partial u}{\partial y} \right)_w \right] \quad (18)$$

if  $l_2 \leq z < l_3, y = y_1$ .

Eq. 10 – 18 can be presented in the dimensionless form for the convenience. Coordinates  $z, y$  are divided by  $y_1$ , velocity components  $u$  and  $v$  - by  $u_0$ , pressure - by the value of dynamic head  $\rho_0 u_0^2$ , temperature  $T$  - by  $\theta_0$ , density, yield point, coefficients of thermal capacity, viscosity, thermal conductivity - by their values at the temperature  $\theta_0$ . A set of equations (10) – (18) in the dimensionless form is presented in Appendix. The equations in the dimensionless form include Reynolds number  $Re$ ,  $Pr$  and  $tl$  number  $Pr$  and Eckert number  $Ec$ .

Set of equations (1) – (13) is solved numerically at boundary conditions of Eq. 14 – 18. The considered zone is broken down into elementary cells with sides  $\Delta z_i, \Delta y_j$ . Difference analogues of the motion equation (10) and energy equation (12) have been obtained by the Crank-Nicolson method of the second order precision, and difference analogue of the equation (11) – by two-layer scheme of the second order precision. Pressure gradient is defined by the splitting method from the condition of flow rate conservation Eq. 13. Pressure gradient is defined by the splitting method from the condition of conservation of mass flow rate (13).

### Discussion of the Calculated Data of the Bushing with Flat Cavity

Calculations were carried out for the slurry with account of rheological properties before and after ultrasonic exposure. In the Fig. 2, the distributions of the temperature and the longitudinal component of the velocity in three thermal contours of the flat bushing at the thickness of the cavity of  $2h = 0.0015$  m and molding velocity of  $u_0 = 1.0$  m/min without (Fig. 2,a) and with (Fig. 2,b) ultrasonic exposure, are demonstrated.

The longitudinal component of the velocity and the temperature of the slurry at the inlet of the channel are constant along the cross-section, which is equal to  $u_0 = 1.0$  m/min. The profile of the longitudinal

component of the velocity attains the shape of shear flow of the fluid near the inlet section due to high viscosity of the thermoplastic slurry (Fig. 2).

Sliding velocity at the wall is almost zero. Wall temperature in the first cooling contour is  $\theta_1 = 73^\circ\text{C}$  and the temperature field is changed from  $75^\circ\text{C}$  to  $73^\circ\text{C}$  in this zone (Fig. 2). Temperature isolines (isotherms) show the zones of the constant temperature and internal structure of the slurry being in liquid state.

Wall temperature is  $\theta_2 = 59^\circ\text{C}$  in the second cooling contour. Dynamic viscosity,  $\mu(T)$ , density,  $\rho(T)$ , and yield point,  $\tau_0(T)$ , increase with decreasing temperature, and viscous-plastic property of the slurry begins to be evident. The slurry slides along the cavity wall, and sliding velocity increases along the length of the second contour during motion down.

It resulted in that profile of the longitudinal component of the velocity down the flow will level with constant center in the near-axial zone (Fig.2). Consequently, the profile of the longitudinal component of the velocity down the flow will level with constant center in the near-axial zone (Fig. 2).

A growth of heat extraction of wall in the second cooling contour leads to a reduction of the temperature field (Fig. 2). There is a transition zone in the beginning of the second contour, where the temperature field is variable expressing the transition of the slurry from the liquid state into the viscous-plastic state. The temperature of the slurry changing from  $73^\circ\text{C}$  to  $59^\circ\text{C}$  defines upper boundary of the zone with constant temperature  $59^\circ\text{C}$ . The slurry is in viscous-plastic state near the wall due to the heat extraction, while the slurry in the central part of the cavity is in a liquid state. The presence of different structural states along the cross-section results in the change of the rheological and thermo-physical properties of the slurry.

The wall temperature in the third cooling contour is equal to  $\theta_3 = 45^\circ\text{C}$ , which leads to the further cooling of the slurry and reduces the temperature from  $59^\circ\text{C}$  to  $45^\circ\text{C}$  in the transition zone.

Further growth of sliding velocity is observed in the third contour. This results in leveling of the longitudinal component of the velocity  $u$  along the cross section of the cavity and there is almost piston-like distribution of  $u$  at the outlet of the bushing (Fig. 2).

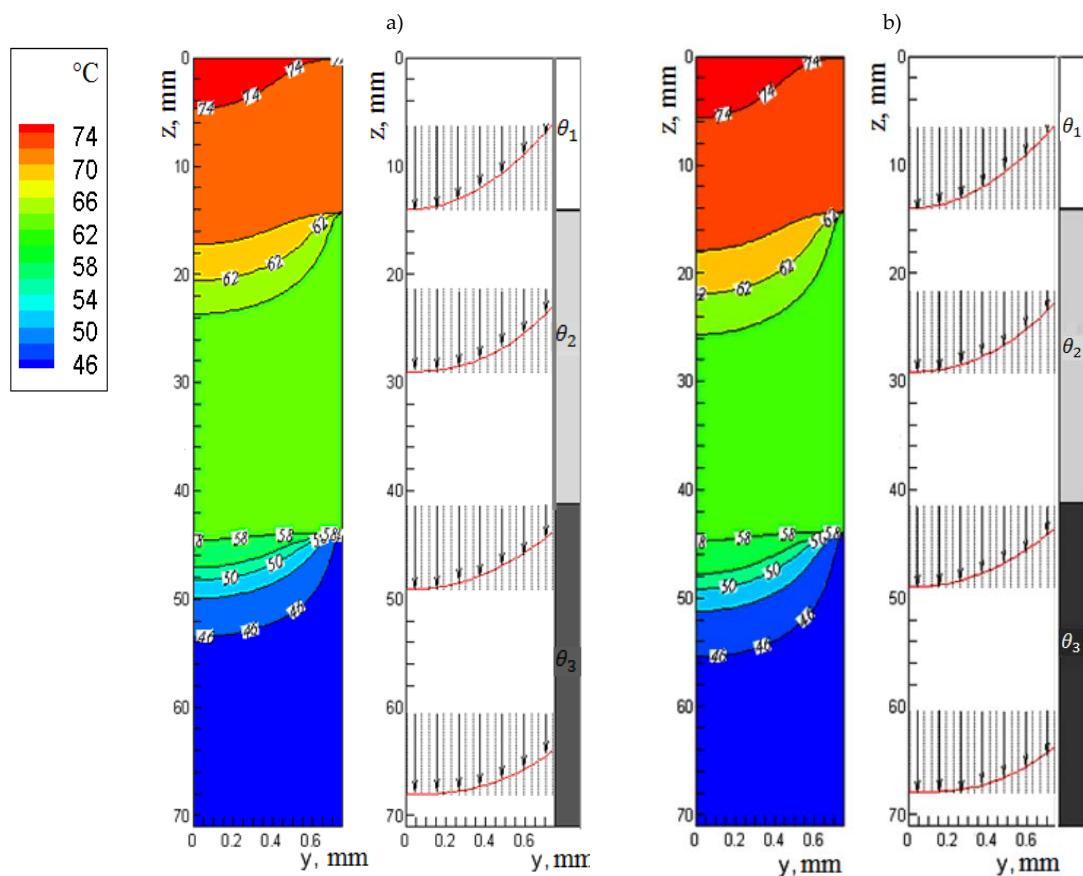


FIG.2 DISTRIBUTION OF THE TEMPERATURE AND LONGITUDINAL VELOCITY IN THE CAVITY WITHOUT (a) And With (b) ULTRASONIC EXPOSURE. INCREASED TRANSITION ZONE OF "GREEN TO BLUE COLOUR" IN (b):

$$y_1 = 0.00075 \text{ m}, u_0 = 1.0 \text{ m/min.}$$

The transition from viscous-plastic state (green zone in Fig. 2) into solid-plastic state (blue zone in Fig. 2) takes place in this zone, where rheological and thermo-physical properties of the slurry are homogeneous.

Comparing the temperature field of the slurry in the cavity without ultrasonic (Fig. 2, a) and with ultrasonic exposure (Fig. 2,b) one may notice the difference in isotherm distributions. Structural change of the slurry occupies more area in the case of ultrasonic exposure (increased transition zones of "green to blue colours" in Fig. 2, b), than that without ultrasonic exposure. It is explained by the increase of the slurry fluidness during ultrasonic exposure due to the change of rheological properties.

Calculation data confirm the experimental fact that, ultrasonic exposure, raising the fluidness of the slurry, reduces the pressure of casting during the formation process to get ceramic fabrications.

Molding velocity  $u_0 = 2.0 \text{ m/min}$  is double increased, which influences the structural change of the slurry;

while the other parameters keep constant (Fig. 3).

Calculation data without ultrasonic exposure (Fig. 3, a) and with ultrasonic exposure (Fig. 3,b) here are also shown. In contrast to the previous regime of formation, the increase of molding velocity leads to the extension of the transition zone of structural changes from one state into another. It is evident from the temperature distribution (Fig.3): the transition zone from liquid state (red) to viscous-plastic state (green) and the transition zone from viscous-plastic state (green) to solid-plastic state (blue).

Transition zones are expanded in the case with ultrasonic exposure, which is explained by a change in rheological properties of slurry and increase of slurry fluidity (Fig.3).

It can be seen from Figures 2, 3 that transition zones have curvilinear convex surfaces with different areas, which can lead to uneven shrinkage of the slurry along the section of the form-building cavity.

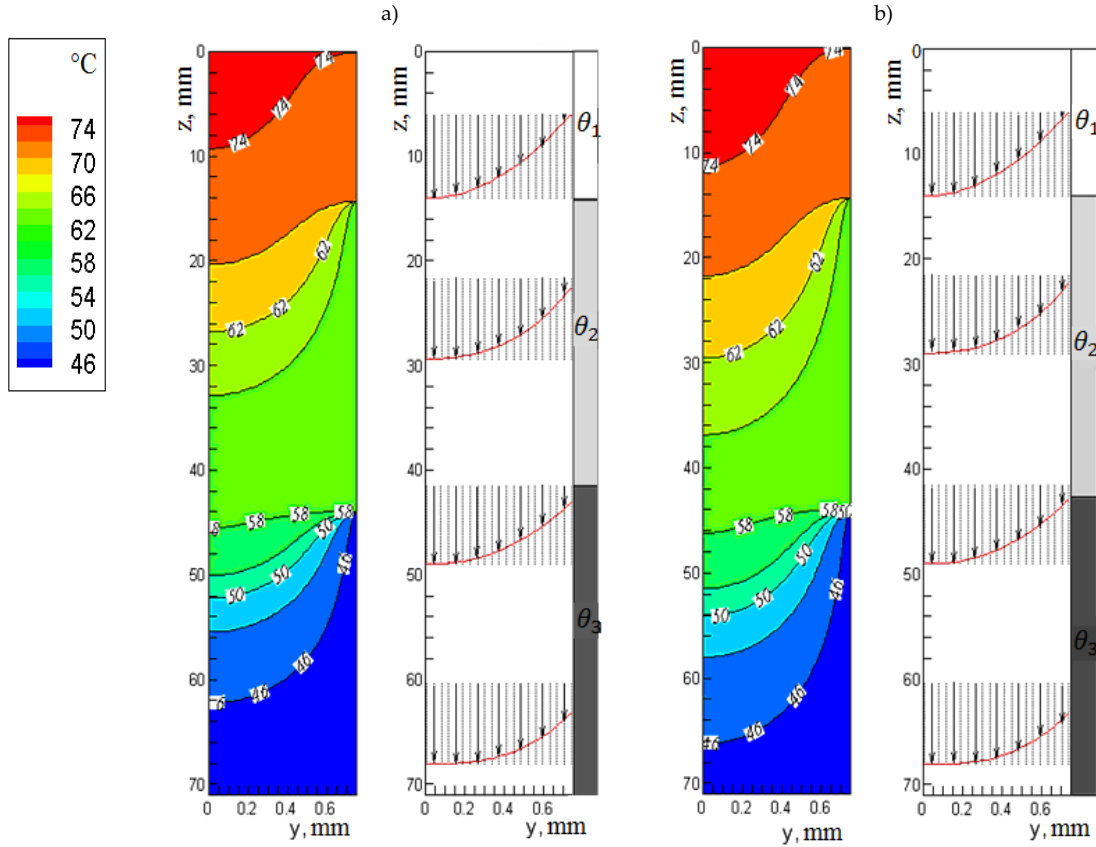


FIG. 3 DISTRIBUTION OF THE TEMPERATURE AND LONGITUDINAL VELOCITY IN THE CAVITY WITH (a) AND WITHOUT (b) ULTRASONIC INFLUENCE. INCREASED TRANSITION ZONES OF "RED TO GREEN COLOUR" AND "GREEN TO BLUE COLOUR" IN (b):  $y_1 = 0.00075$  m,  $u_0 = 2.0$  m/min

The density of thermal flow at the wall describing a heat exchange between the slurry and the wall of cavity can be expressed as:

$$q_w = -\lambda \left( \frac{\partial T}{\partial y} \right)_w \quad (19)$$

Variation of the density of thermal flow by the length of the cavity of flat bushing is shown in the Fig. 4, where  $q_{w0}$  is density of thermal flow at the initial temperature of slurry  $\theta_1 = 75^\circ\text{C}$ .

The wall temperature in the first cooling contour is  $\theta_1 = 73^\circ\text{C}$ , and a small change of thermal flow density  $q_w$  at wall is observed, which is due to minor difference between the initial temperature of the hot slurry  $\theta_0$  and the wall temperature  $\theta_1$ . The reduction of wall temperature till  $\theta_2 = 59^\circ\text{C}$  in the second cooling contour leads to a sharp increase of thermal flow density  $q_w$  in the narrow area of transition zone due to uneven reduction of the wall temperature from  $\theta_1 = 73^\circ\text{C}$  to  $\theta_2 = 59^\circ\text{C}$ .

Downwards by the direction of the motion, thermal flow density,  $q_w$ , steadily approaches zero due to leveling of the slurry temperature field.

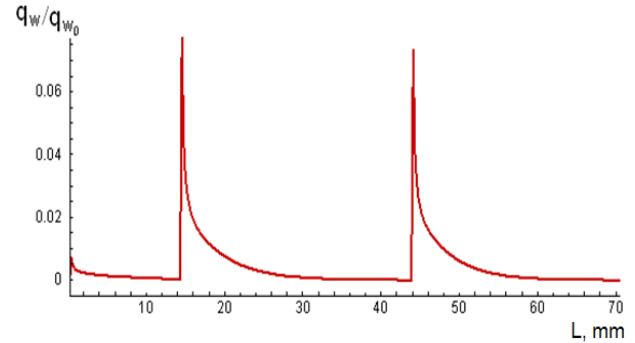


FIG. 4 CHANGE OF THE THERMAL FLOW DENSITY AT THE WALL ALONG THE LENGTH OF THE CAVITY:  $y_1 = 0.00075$  m,  $u_0 = 1.0$  m/min

Thermal flow density,  $q_w$ , in the third cooling contour changes similarly due to abrupt reduction of the wall temperature from  $\theta_2 = 59^\circ\text{C}$  to  $\theta_3 = 45^\circ\text{C}$  with a monotonic decrease by leveling of temperature field.

Process of transition of the slurry from one structural state into another in the cavity can be also analyzed through the change of the density. Change of the slurry density along the length of the axial plane of the cavity is demonstrated in the Fig. 5, where  $\rho_0$  is slurry density at the initial temperature  $\theta_0 = 75^\circ\text{C}$ .

A change of density along the first cooling contour is small, i.e. the slurry maintains the initial liquid state. In the second contour, density of the slurry increases by 1.9% and is stable all the way of this part, i.e. a transition of the slurry from liquid state into viscous-plastic state takes place. Density of the slurry increases by 2.2% in the third contour, the slurry is hardened and turned from viscous-plastic state into solid-plastic state.

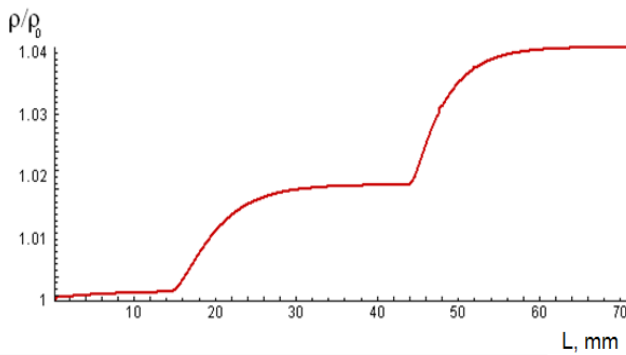


FIG. 5 CHANGE OF THE DENSITY OF THE SLURRY ALONGTHE LENGTH OF THE CAVITY:  $y_1 = 0.00075$  m,  $u_0 = 1.0$  m/min

#### Comparison: Calculation versus Experiment

Specific surface area of the powder described in Table 1 has an optimal value to obtain the ceramic fabrications with good soundness. Experiments show that at other values of specific surface area of the powder, weight content of binder increases or a destruction of ceramic occurs due to a presence of micropores and fractures. Experimental data of slurry viscosity and values of molding capacity, molding velocities for different weight fractions of binder in slurry presented in Table 2 are obtained for the formation process in flat cavity (Fig. 1).

TABLE 2 CERAMIC SOUNDNESS DEPENDENCE ON MOLDING VELOCITY IN A FLAT CAVITY WITHOUT ULTRASONIC EXPOSURE

Binder content in slurry, weight fraction	Slurry viscosity at $\theta_0 = 75$ °C, Pa*s	Molding capacity of slurry, mm	Molding velocity, mm/min	Mechanical soundness of casting at bend, mPa
0.095	7.23	23	193	9.53
0.100	6.10	35	185	9.33
0.107	4.80	55	177	8.85
0.112	4.47	72	171	8.41
0.117	4.17	89	165	8.17

These data indicate that there is an optimum value of molding velocity, corresponding to each weight

content value of binder, which provides mechanical soundness of casting during formation process. Mechanical soundness of casting increases with molding velocity (Table 2). Maximum value of mechanical soundness of casting of 9.53 mPa corresponds to the molding velocity of 193 mm/min and weight content of binder of  $\omega = 0.095$ .

Calculation data on velocity and temperature (Fig. 2, 3) are obtained at binder weight fraction of  $\omega = 0.117$ . In order to carry out the calculations at other values of binder, empirical formulas of coefficient of plastic viscosity  $\mu$  and yield point  $\tau_0$  on temperature have to be known.

For instance, for binder weight fraction of  $\omega = 0.1$ , empirical formulas of coefficient of plastic viscosity,  $\mu$ , and yield point,  $\tau_0$ , on temperature have the following form:

before US exposure

$$\mu(T) = 5.5 + 6.2 \cdot \exp(-(T - 334)/6), (\text{Pa} \cdot \text{s})$$

$$\tau_0(T) = 19 + 11.41 \cdot \exp(-(T - 340)/5.47), (\text{Pa})$$
(20)

after 28 min US exposure

$$\mu(T) = 2.5 \cdot 10^{14} \cdot \exp(-0.09068 \cdot T), (\text{Pa} \cdot \text{s})$$

after 15 min US exposure

$$\tau_0(T) = 5.93 \cdot 10^8 \cdot \exp(-0.04968 \cdot T), (\text{Pa}) \quad (21)$$

Binder density for  $\omega=0.1$  is defined by the formula:

$$\rho_{cb}(T) = 0.8485 +$$

$$+ 0.0755 \cdot \cos(0.0571 \cdot T - 16.736), \left( \frac{\text{g}}{\text{cm}^3} \right) \quad (22)$$

The solution to a set of equations (10) – (18) along with (20) - (22) calculation data on the forming process of slurry with binder weight fraction of  $\omega = 0.1$  can be obtained.

The next calculation data on temperature were obtained for flat cavity at two molding velocity values:  $u_0 = 0.185$  m/min (Fig. 6,a) and  $u_0 = 0.165$  m/min (Fig. 6,b). These molding velocities correspond to weight content values of binder  $\omega = 0.1$  and  $\omega = 0.117$ , respectively (Table 2).

As seen from Figure 6 the transition zones between cooling contours occupies small areas. Molding velocities of  $u_0 = 0.185$  m/min and  $u_0 = 0.165$  m/min, provide uniform temperature distribution along the section of flat cavity. Uniform distribution results in homogeneous rheological and thermo-physical

properties of the slurry along the section of flat cavity. In this case the shrinkage of slurry is small and uniform along the section of cavity. Therefore no blisters and cavities are formed, which leads to soundness failure of beryllia casting.

The slurry completely is solidified in the form-building cavity, which may mean that ceramic fabrication of beryllia (BeO) totally attains constructive form for further treatment.

Use of hot molding method for slurries of aluminum oxide, zirconium dioxide, calcium oxide and magnesia oxide is mentioned in references. The mathematical model can be applied to form process of slurries of aluminum oxide, zirconium dioxide, calcium oxide and magnesia oxide. The calculations require the empirical dependences on temperature of thermo-physical features of slurries of aluminum oxide, zirconium dioxide, calcium oxide and magnesia oxide.

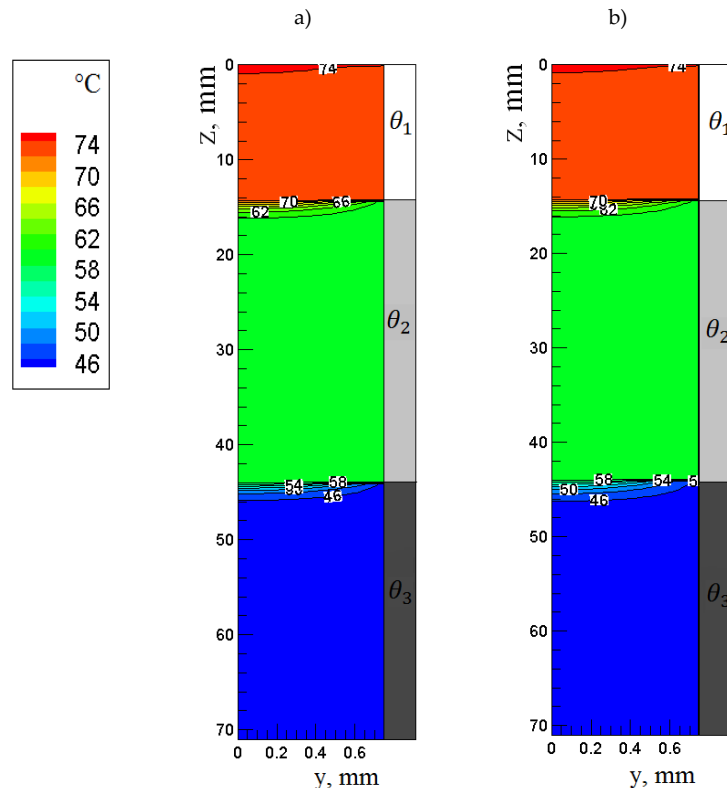


FIG. 6 TEMPERATURE DISTRIBUTION IN A FLAT CAVITY DEPENDING ON MOLDING VELOCITY: a)  $u_0 = 0.185$  m/min; b)  $u_0 = 0.165$  m/min

## Conclusion

Investigation results show that the mathematical model describes all the stages of the ceramic molding including the changes of aggregate state. Ultrasonic exposure enhances the rheological properties and increases the fluidity of the thermoplastic slurry in the form-building cavity. All the stages of the hot molding method of the thermoplastic slurry (liquid state, viscous-plastic state, solid-plastic state) can be presented by the changes of the longitudinal velocity and temperature along the length of the cavity. Density of heat flow at the wall of the form-building cavity changed in accordance with the boundary conditions expresses heat extraction at the wall.

The slurry density increases during the transition from the liquid state into viscous-plastic and solid-plastic states. Such a density distribution in a satisfactory compliance with the experiment expresses balancing mechanism of volumetric changes of the slurry.

Optimum conditions of the ceramic molding process by the hot molding method can be found with calculations, which will allow obtaining the hardened fabrication with homogeneous structure of beryllia at the outlet.

## REFERENCES

Akishin, G.P., Turnaev, S.K., Vaispapir, V.Ya., Gorbunova, M.A., Makurin, Yu. N., Kiiko, V.S., Ivanovskii, A.L.

"Thermal conductivity of beryllium oxide ceramic." Refractories and Industrial Ceramics 50 (2009): 465-4.

Akishin, G. P., Turnaev, S. K., Vaispapir, V. Ya., Kiiko, V. S., Shein I. R., Pletneva E. D., Timofeeva M. N., Iva A. L. "Composition of beryllium oxide ceramics." Refractories and Industrial Ceramics 11 (2011): 377-5.

Anderson, J.D., Tunnehill, J.C., and Pletcher, R.H. "Computational Fluid Mechanics and Heat Transfer." Moscow: Mir, 1990. [Russian transl.]

Cebeci, T. and Bradshaw, P. "Physical and Computational Aspects of Convective Heat Transfer." Moscow: Mir, 1987. p. 592 [Russian translation]

Dobrovolskii, A.G. "Slurry Casting." Moscow: Metallurgiya, 1977. [in Russian]

Dvinskikh, Yu.V., Popil'skii, R.Ya., Kostin, L.I., Kulagin, V.V. "Thermophysical properties of thermoplastic casting slips of some high-refractory oxides." Ogneupory 12 (1979): 37-4. [in Russian]

Shakhov, S.A. "Controlling the deformation behavior of thermoplastic slips with ultrasound." Glass and Ceramics 64 (2007): 354-3.

Shakhov, S.A. "Use of ultrasound in order to intensify molding of high-temperature thermocouple sheaths." Refractories & Industrial Ceramics 49 (2008): 261-3.

Shakhov, S.A., Bitsoev, G.D. "Application of Ultrasound in the Manufacture of High Thermal Conductivity Ceramic Articles." Ust'-Kamenogorsk: EKTU, 1999. [in Russian]

Shakhov, S.A., Gagarin, A.E. "Rheological characteristics of thermoplastic disperse systems treated with ultrasound." Glass and Ceramics 65(2008):122-3.

Zhabasbayev, U.K., Ramazanova, G.I., Sattinova, Z.K. "Mathematical model of hot-cast molding of ceramic." Glass and Ceramics 68 (2011): 216-5.

Zhabasbayev, U.K., Kaltayev, A., Bitsoyev, G.D., Turnayev, S.K. "Hydrodynamics of moulding of ceramic articles for beryllia with ultrasonic activation." Proceedings ASME International Mechanical Engineering Congress and Exposition. Orlando, 2005; 177.